NOLTR 61-121

SPALL STUDIES IN COPPER

NOL

28 DECEMBER 1961

UNITED STATES NAVAL ORDNANCE LABORATORY, WHITE OAK, MARYLAND

20060608049

SPALL STUDIES IN COPPER

Prepared by:

R. A. Plauson, J. Grimsley, and A. D. Solem

Approved by: _J Kab.k,_
Chief, Explosion Dynamics Division

Edmund Adams
Chief, Magnetism and Metallurgy Division

ABSTRACT: A gas gun system for use in studying one-dimensional spall conditions in thin metal plates is described. This gun is capable of producing well controlled plane impact of a "missile" disc 1.69 inch in diameter on a "target" disc of adjustable diameter at velocities up to 150 meters per second. Missile and target thicknesses can be varied as required in the experiments.

This system has been applied to determine minimum conditions to produce spall in copper. For missiles of $\sim$0.10-inch thickness and targets of $\sim$0.20-inch thickness spall occurs as follows:

Material	Impact Velocity (m/sec)	Tension Pressure (kbars)
Annealed bar	138	48
Annealed plate	61	22
1/4-hard plate	72	26
Hard plate	57	19

It is concluded that spall and the nature in which it forms as functions of impact conditions, depends principally on the material form (i.e., bar or plate). The material condition (i.e., annealed, 1/4-hard or hard), was found to have a relatively small effect.
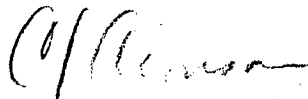
W. D. COLEMAN
Captain, USN
Commander

C. J. ARONSON
By direction

L. R. MAXWELL
By direction

CONTENTS

Page

ILLUSTRATIONS

ILLUSTRATIONS (Con't)

SPALL STUDIES IN COPPER

INTRODUCTION

1. When a metal plate (or any solid plate, for that matter) is subjected to an intense pressure pulse or shock on one side, material from the opposite surface may be spalled or scabbed free. Such a pressure pulse might be generated by explosive attack or by high-speed impact. The spalling can range from microscopic internal cracking of the plate to the ejection of a considerable portion of the free surface at relatively high velocities*. Failure by spalling results if the stresses introduced can develop into tensions that exceed the dynamical tensile strength of the material. When spall does occur in a plate, there is a drastic reduction in strength. A knowledge of conditions under which spalling can occur is thus significant in the design of any system that might be subjected to shock environments.

2. In the past, concern for spall centered principally around massive plates, and spall studies were directed toward establishing conditions under which steel armor several inches thick could or could not be breached by explosive attack. Now, however, with the development of missile systems, the concern for spall has become critical for all materials that for one reason or another might be considered for application in missiles. Such systems must be designed precisely to optimize performance.

3. An investigation to study the basic aspects of spall has been under way at the Naval Ordnance Laboratory since 1959. This work has been directed toward:

> Establishing the minimum conditions under which spall would be produced.

> Relating spall to the physical, mechanical, and metallurgical properties of materials.

> Studying mechanism of spall and hardening induced in materials by one-dimensional shocks of low amplitude.

The approach in this work has been generally to develop equipment and techniques for proper control of conditions under which spall could be generated and then investigating systematically

---

*Under conditions of high intensity attack the plate may be breached or penetrated.

spall in a limited number of materials. The choice of material and test geometry was to be such that the information developed would be useful in missile design problems.

4.   In this work it has been found that adequate control can be obtained only by solid impact on the material to be spalled and that minimum pressure amplitudes to produce spalls are so low that gas gun acceleration is the most satisfactory means of producing the impact. It has also been found that a high degree of refinement is needed, both in control of the specimens and the experiments, to assure satisfactory results. This report describes the gas gun system and the appropriate experimental techniques for study of spall. It also discusses the observations to date and interpretations of spall in copper.

SPALL

5.   Spall from the free surface of a solid can be simply described from fluid dynamical considerations in which the assumed fluid character of the material is modified by the concept of particle separation of a scabbing nature in the presence of negative pressures or tensions which exceed some limiting value characteristic of the material. It must occur whenever particle velocity discontinuities of an expansive nature above some critical value develop in the solid material. Typical spalling situations can occur with the collision of shock waves or the meeting of rarefaction waves. The impact of metal plates with subsequent development of shocks and the interaction of rarefaction waves to produce spall, as used in the experiments, will be given as an example of the process.

6.   Consider the one-dimensional impact of a thin "missile" plate upon a somewhat thicker "target" plate of the same material at a velocity u. (It is assumed that the impact is sufficiently strong to produce spalling.) Figure 1 indicates the process at various times.

> Before impact both plates are at normal pressure and density (Figure 1a).

> At time of impact at velocity u a pressure develops at the interface of a value characteristic for the material at this impacting velocity (1) (Figure 1b).

> The interface starts moving forward with velocity $\sim u/2$ and shocks travel forward into the target plate and backward into the missile plate at velocities U dependent on the material and the amplitude of the pressure. Behind these shocks material particles will be moving with velocity $\sim u/2$ (Figure 1c).

RAREFACTION

PARTICLE VELOCITY
u/2 →

U_R

U_R

PARTICLE VELOCITY IN
THIS REGION IS u →

RAREFACTION

PARTICLE VELOCITY IN
THIS REGION IS 0

(e) RAREFACTION WAVES WITHIN
TARGET PLATE

RAREFACTION
WAVES
COLLIDE

PARTICLE VELOCITY IN
THIS REGION IS u →

PARTICLE VELOCITY IN
THIS REGION IS 0

(f) RAREFACTIONS COLLIDE

SEPARATION
OCCURS

PARTICLE VELOCITY IN
THIS REGION IS u →

PARTICLE VELOCITY IN
THIS REGION IS 0

(g) SEPARATION

TARGET PLATE

MISSILE PLATE

u

(a) BEFORE IMPACT

(b) AT IMPACT

SHOCK IN TARGET PLATE

SHOCK IN MISSILE PLATE

u

u

INTERFACE

PARTICLE VELOCITY IN THIS
REGION IS 0 →

PARTICLE VELOCITY
IN THIS REGION IS u

PARTICLE VELOCITY IN THIS REGION IS u/2 →

(c) SHOCK IN PLATES

SHOCK IN TARGET PLATE

U

U_R

R

u=0

u/2

u=0

u=0

PARTICLE VELOCITY IN THIS REGION IS u/2 →

RAREFACTION WAVE IN MISSILE
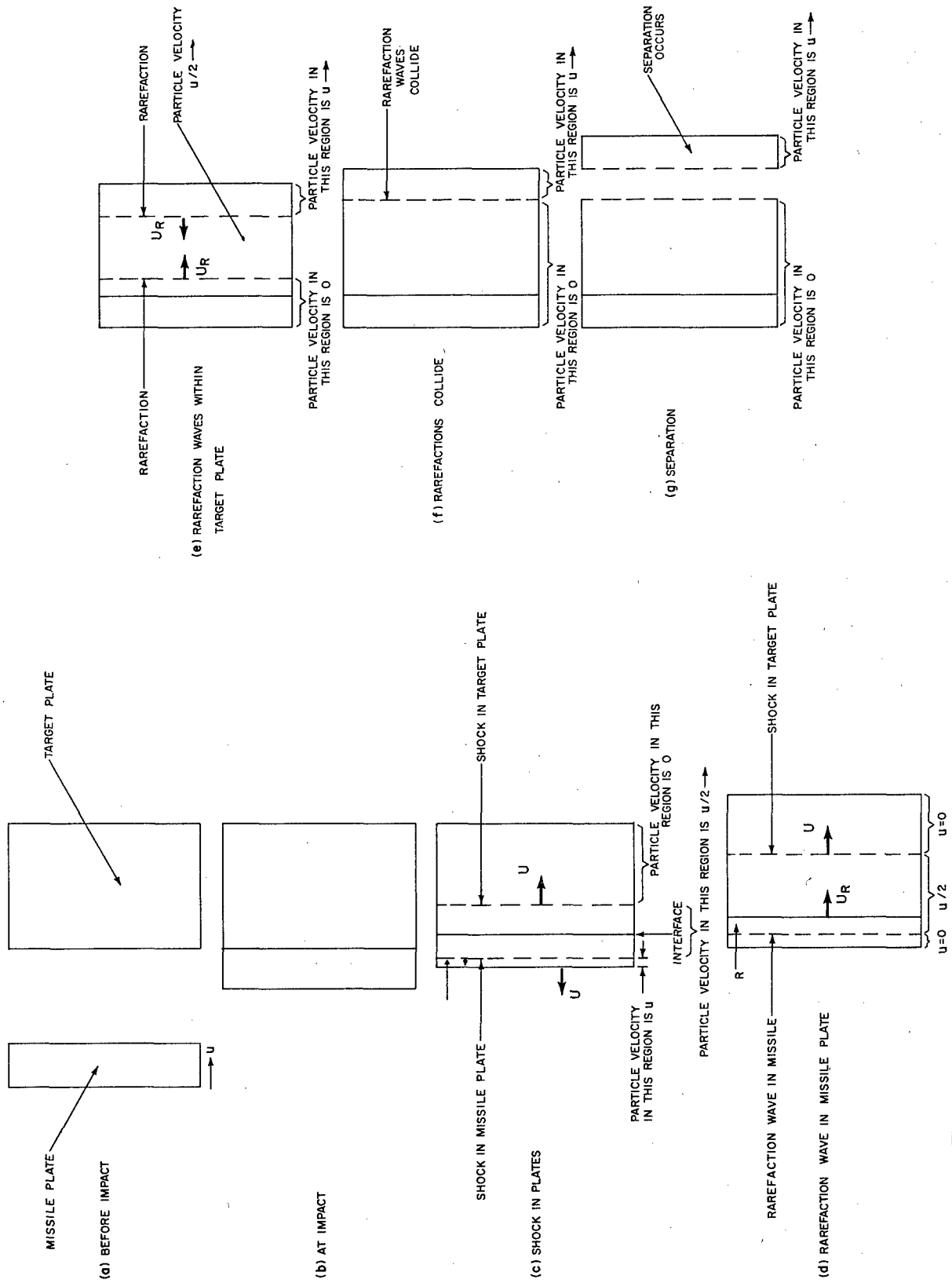
(d) RAREFACTION WAVE IN MISSILE PLATE

FIG. I   PRODUCTION OF SPALL THROUGH THE ONE-DIMENSIONAL IMPACT OF TWO METAL PLATES

The shock wave in the "missile" plate arrives at the free surface and is reflected as a rarefaction wave moving toward the interface between the two plates. The particles behind this wave are at rest (a change in velocity of u/2 (Figure 1d)).

The shock wave in the "target" plate arrives at the free surface and is also reflected as a rarefaction wave moving back toward the interface. Particle velocity behind this wave has amplitude u moving in a direction opposite to the direction of the rarefaction wave (Figure 1e).

The rarefactions meet on a plane in the target plate. The material on one side of the plane is at rest; the material on the other side is moving with velocity u. Separation occurs as spall (Figures 1f and 1g).

7   The example of spall produced by metal plate impact is relatively clean. A square pressure pulse is in effect applied to the specimen and the fracture that results is normally in a well defined location and of a nature dependent upon the structure and geometry of the material being investigated.* Spalling produced by explosive attack might well not be so clearly defined. The pressure pulse is spiked with rapid decay in time. Such a pulse applied to the specimen could produce spalls or spalling situations of varying degrees on a variety of closely spaced planes in the specimen that could result in highly irregular separation (2).

EQUATION OF STATE CONSIDERATIONS

8.   There is abundant information available on both the static and dynamic compressive equations of state for many materials (1), (3), and (4). However, there is little or no data of equation of state nature pertaining to the dynamic tensile behavior of solids. Hence, it is difficult to describe the conditions a solid undergoes while unloading from pressures produced by impulsive loads. One approach to provide pressure-density or pressure-particle-velocity relationships to describe the behavior of the materials when subjected to negative pressures or tensions is to extend the well known compressive, shock Hugoniot, equations of state into the third quadrant of the

---

*This condition holds only up to the time the material commences yielding. As spalls start to form the material is no longer supporting the original tensile forces.

pressure-particle-velocity plane as shown in Figure 2. This may be done in any number of ways. As a straight forward approach one may

Extend the pressure-particle velocity relationship which holds for densities greater than normal into the region where densities are lower than normal (Graph c of Figure 2).

Extend only the first order term of this relationship into the region of lower than normal densities (Graph b of Figure 2).

Consider the pressure-particle-velocity relationship for lower than normal densities (material under tension) as a mirror reflection through the point P = 0 u = o as an origin (Graph a of Figure 2).

9. Figure 2 shows the comparison of these possibilities for copper. At densities much lower than normal the tension (negative pressure) one would predict for a given particle velocity would be critically dependent upon the relationship between pressure and density used. However, for negative pressures only slightly less than zero or densities only slightly below normal conditions it would seem to make very little difference as to how the equation of state is extended into the tension region. At tensions on the order of 17.5 kilobars or less (particle velocities of 0.04 mm/μ second, or less) the three extrapolations of the pressure-particle velocity relationship give nearly identical values. Definite spalls are produced in copper at tensions of this value. It would seem then that the choice of equation of state to describe the fluid dynamic character of copper in a tension state is not critical. It is only necessary that the negative pressure or tension at which spall or material separation occurs be known.

EXPERIMENTAL DETAILS FOR THE STUDY OF SPALL

10. The basic plan of the experiments is to impact, under one-dimensional conditions, a disc of the material to be studied (target disc) with a missile disc. A gas gun accelerates this missile disc, carried in an appropriate sabot (termed the projectile) to the desired test impact velocities. After impact both the missile and target discs are recovered for analysis.

The Gas Gun

11. The gas gun consists essentially of two main parts: the propulsion system, and the observational section. The propulsion system (Figure 3) incorporates three parts:
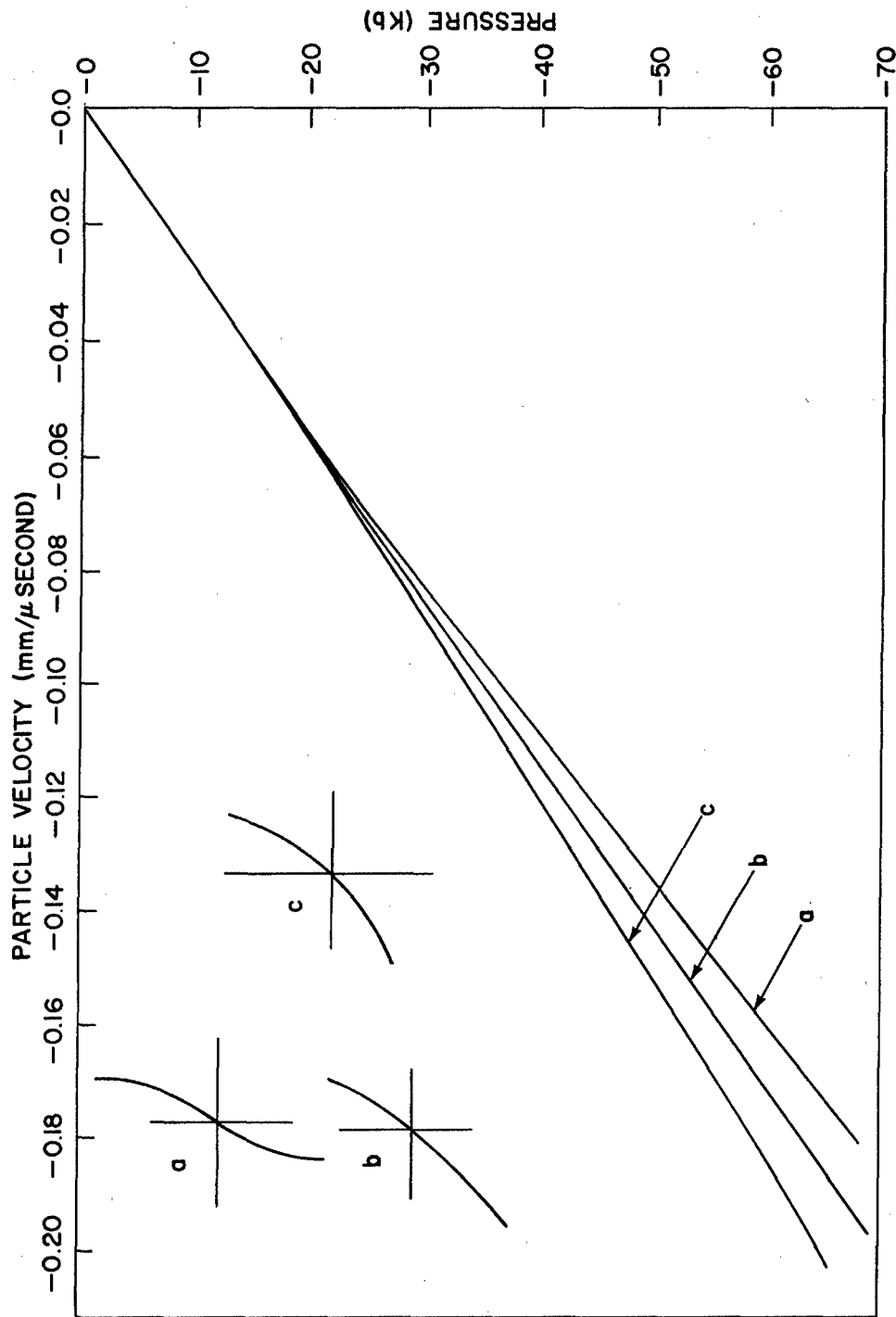
FIG. 2 EXTENSION OF EQUATION OF STATE INTO THE TENSILE REGION

COMPRESSED
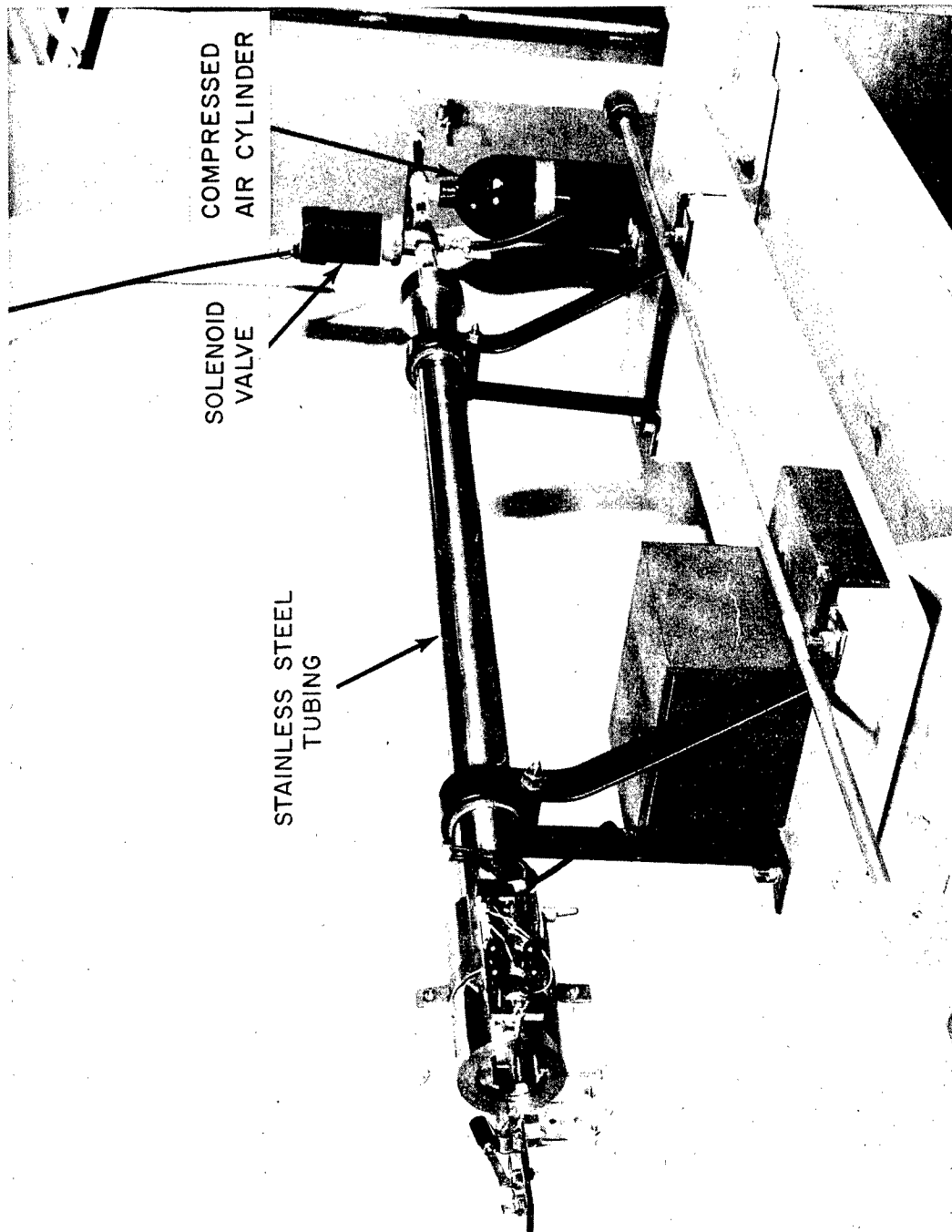AIR CYLINDER

SOLENOID
VALVE

STAINLESS STEEL
TUBING

FIG. 3 GAS GUN CONSTRUCTED FOR SPALL STUDIES

A type D medical compressed-air cylinder for the driving gas reservoir.

A 48-inch section of stainless steel tubing having an I.D. of 1.731 inches for the acceleration chamber.

A 3/8-inch pilot operated solenoid valve which regulates the flow of driving gas from the reservoir to the acceleration chamber.

The driving gas chamber is charged before each firing from bottled gas supply and the pressure of gas delivered to the chamber is regulated by a standard manifold.

12. The driving gas and the gas pressure are selected dependent upon terminal projectile velocity requirements for a given experiment. When the reservoir is charged with helium at a pressure of 1,000 psi, the gun will accelerate a projectile weighing 100 grams to approximately 150 m/second. This represents the upper limit of capability designed for the system since it was developed primarily for low velocity impacts. An experimentally determined calibration curve which is used as a guide in selecting the driving gas pressure to be used for a particular terminal velocity is shown in Figure 4.

The Observational Section

13. The observational section, or muzzle piece of the gun, shown in Figure 5, was designed with three main considerations in mind. These are:

To hold the target (specimen) piece in the proper position for impact by the missile.

To allow an escape route for air which could otherwise be compressed between missile and target prior to impact.

To determine the projectile's velocity just prior to impact.

14. Positioning the target so that its impact face is normal to the axis of the acceleration chamber is accomplished through the use of a flat locating plate shown in Figure 5. To mount the target at the muzzle, the target (held in position by four stubs) is placed in contact with the locating plate. This assembly is then slipped into the muzzle piece whose face is accurately machined normal to the axis of the system. When the target has been aligned properly it is secured in place by four plastic rods under normal screw pressure. Figure 6 shows the steps of this process. As will be discussed later, it is highly critical that the direction of impact be normal to the target face. Great pains with the procedure described above are therefore required to insure proper mounting.
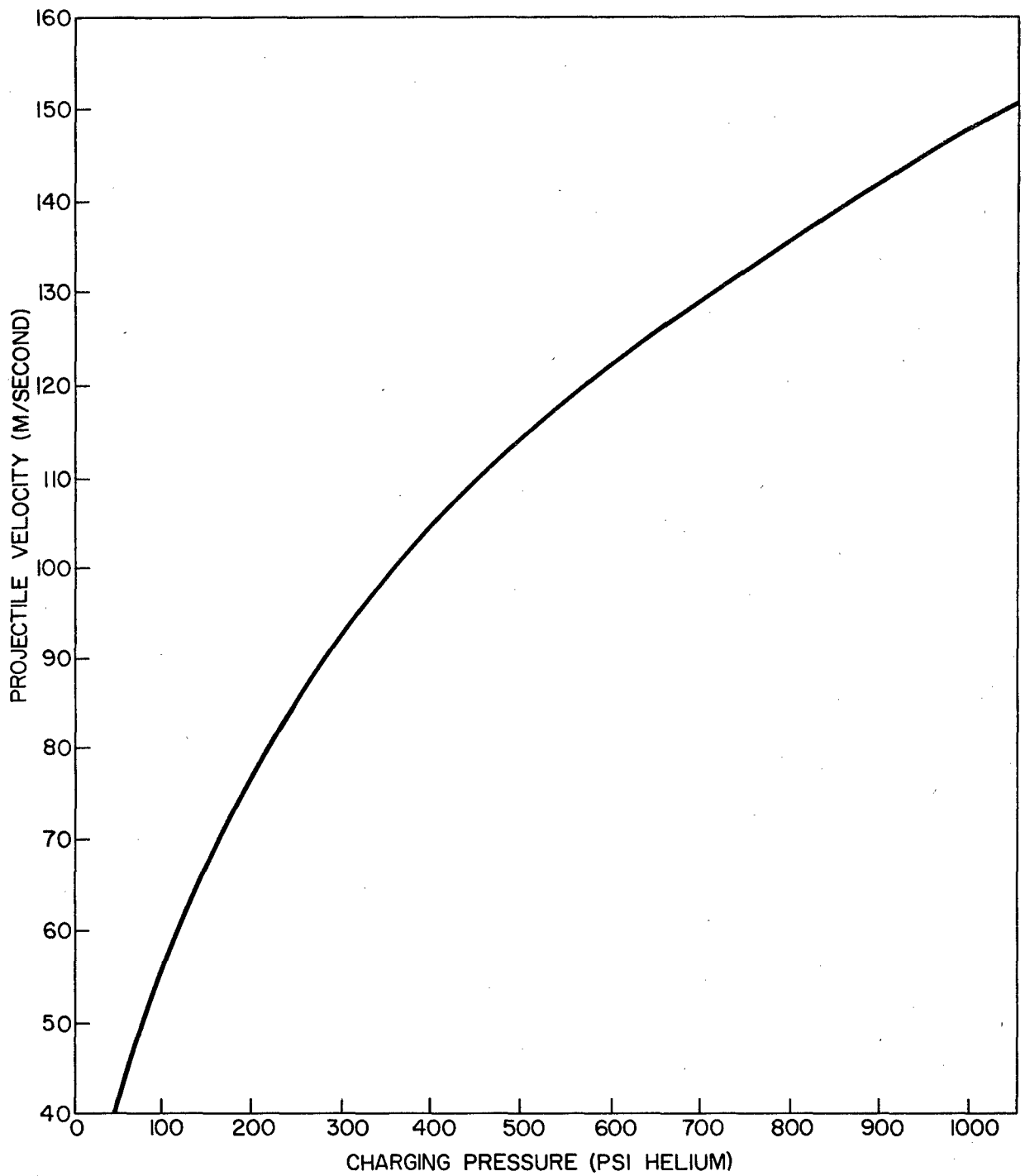
FIG. 4   GAS GUN CALIBRATION FOR 100 gm PROJECTILE USING HELIUM AS
THE DRIVING GAS

WINDSCREWS

PLASTIC RODS

REMOVABLE LOCATING PLATE

TARGET

VENTING SLOTS

ELECTRICAL CIRCUIT FOR VELOCITY DETERMINATION
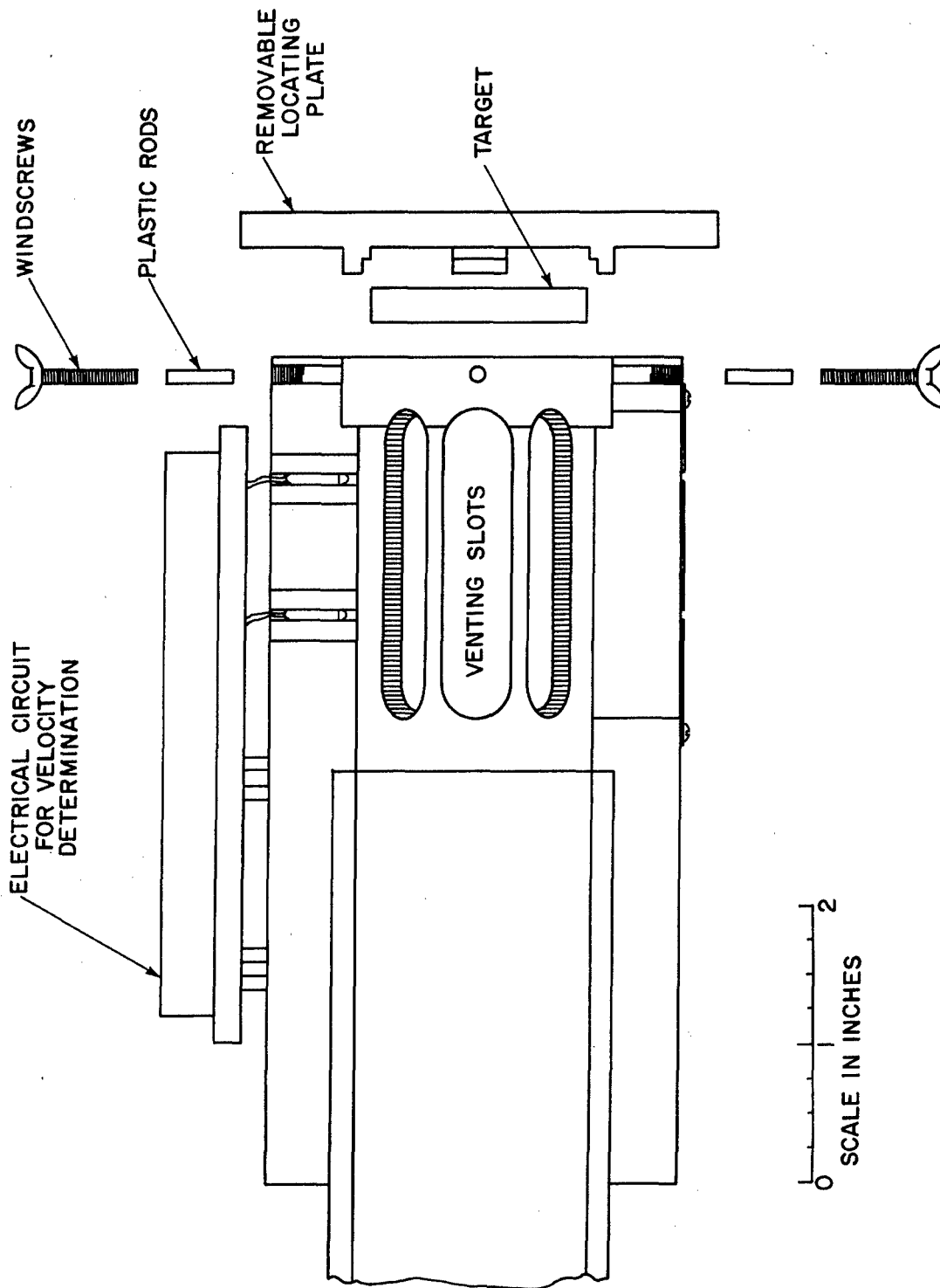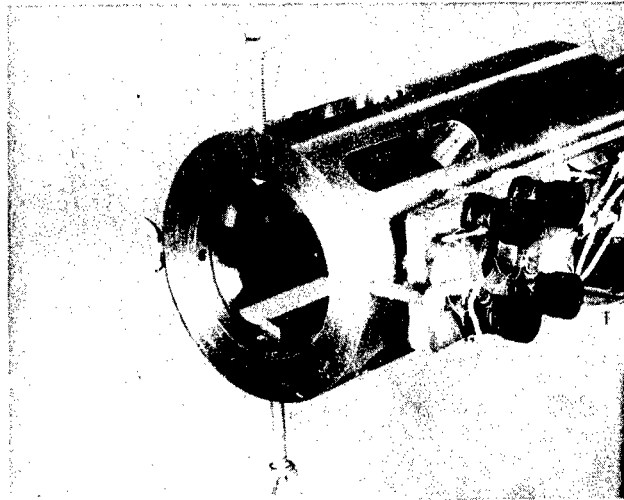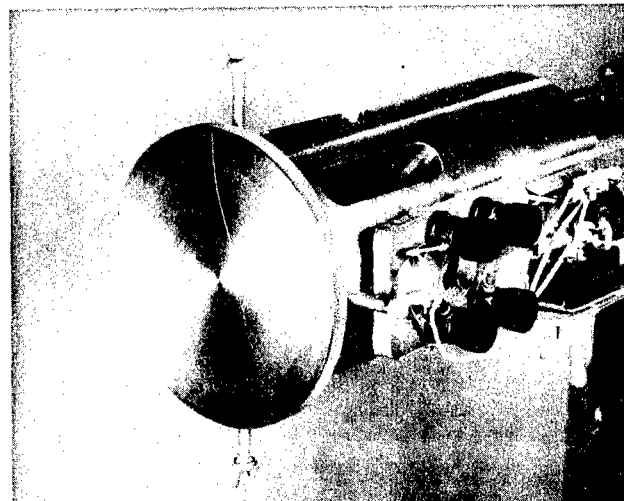
SCALE IN INCHES

FIG. 5 OBSERVATIONAL SECTION OF GAS GUN

(a.) BEFORE
  MOUNTING
   TARGET

(b.) LOCATING
   PLATE ON
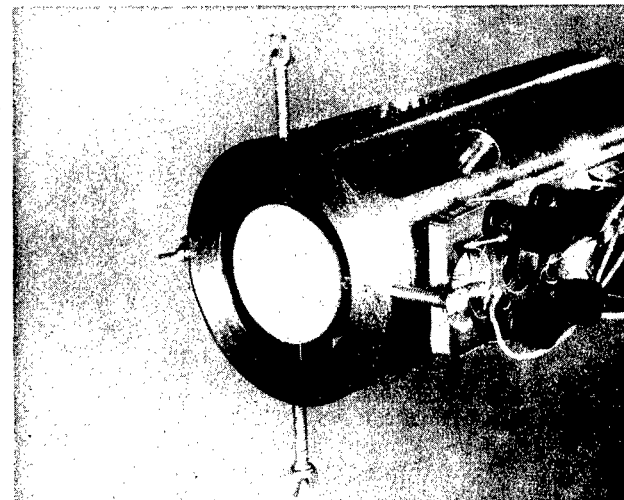 MUZZLE FACE

(c.) TARGET
   POSITIONED
  FOR TESTING

FIG. 6 STEPS IN MOUNTING THE TARGET PLATE

15. The column of air pushed ahead of the projectile is vented through the six lengthwise slots and the annular opening between muzzle and target as seen in Figure 6c. While this may not completely eliminate the presence of compressed air between missile and target prior to impact, at least the volume of air present which is raised to a pressure above atmospheric will be minimized.

16. The projectile's velocity just prior to impact is determined by timing its passage through a precisely known distance (25.43 mm). Two IN2175 photo sensitive diodes are placed at the extremities of this distance interval. Beams of light from across the muzzle illuminate these diodes through appropriate collimating aperatures. As the projectile interrupts these beams of light, signals are generated which are displayed upon a calibrated oscilloscope (Tektronix 551) and photographed. The first signal triggers the scope. The time of transit across the measured distance is obtained from the trace produced by the second signal. Figure 7 shows a typical record. Velocities determined in this way are accurate to within ±1 percent.

The Projectile.

17. A typical test projectile is shown in Figure 8. A 3.00-inch section of 1.730-inch O. D. aluminum tubing having a wall thickness of 0.060 inch serves as a sabot when a plastic tailplug closes the rear end. The forward end of the sabot contains a recess 0.062-inch deep and 1.690-inch I. D. for the purpose of supporting the missile disc to be used in each experiment. (The thickness and shape, other than O. D., of this piece may easily be varied to meet the needs of a particular experiment.)

Recovery.

18. The spent hardware, missile disc, and target are collected in loose sawdust after impact.

ERRORS

19. Errors in the experiment arise chiefly from two main considerations. These are:

Error in determining velocity of projectile just prior to impact.

Error introduced through deviations from design standards which affect the simultaneity of the meeting of rarefaction wave fronts within the specimen material.

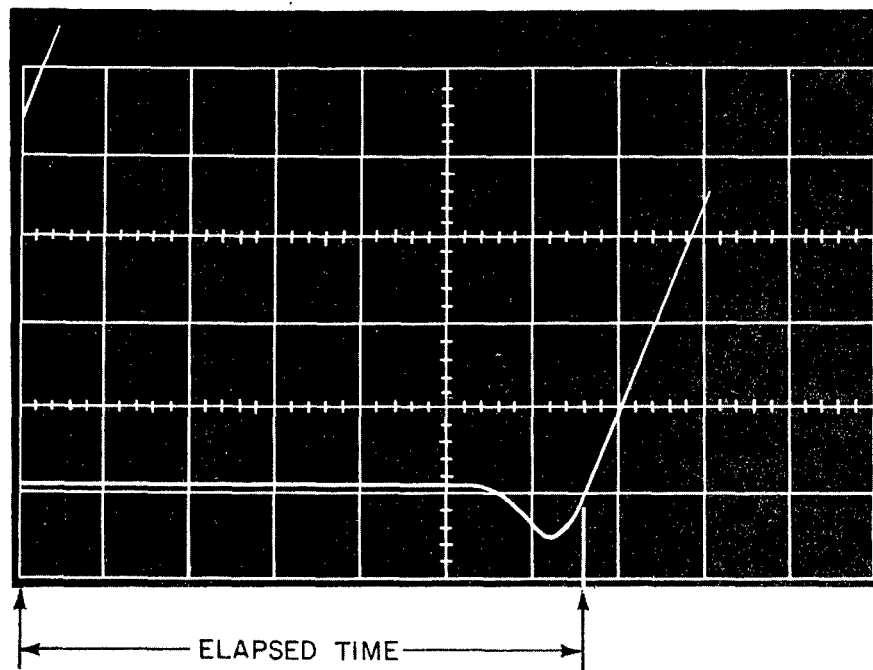ELAPSED TIME

FIG. 7 TYPICAL OSCILLOGRAM, SWEEP SPEED
50 μ SECOND/LARGE DIVISION

PLASTIC
TAIL
PLUG

SABOT

MISSILE

L___|___|___|___|___|___|___|___|

0   I   2
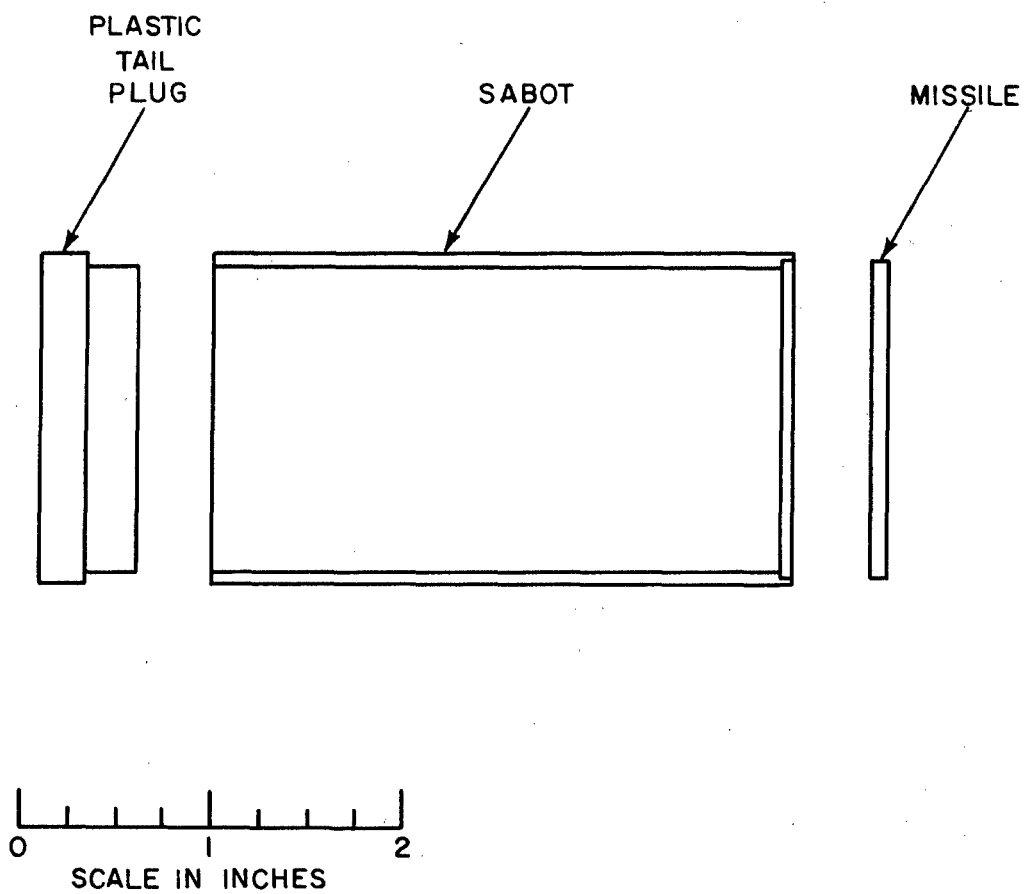
SCALE IN INCHES

FIG. 8   TYPICAL TEST PROJECTILE

20. It is believed that the measurements involved in determining the velocity are sufficiently accurate to place a limit of variation of ±1 percent upon the values given.

21. Of paramount importance is the deviation from one-dimensional impact. The factors which influence the planeness of impact are (along with the amount of angular deviation each can contribute):

Failure to locate target face in a plane parallel to the muzzle face: 0° 1' 4"

Non-parallelism of missile faces: 0° 0' 13"

Non-parallelism of target faces: 0° 0' 13"

Projectile-gun-bore clearance under conditions of maximum allowable tolerance: 0° 3' 26"

Uneven film of adhesive under missile disc in the sabot recess: 0° 0' 13"

The maximum possible angular deviation from one-dimensional impact: 0° 5' 9".

22. At a velocity of impact of 100 meters per second with all of these errors adding, the deviation from simultaneous impact of the missile plate's surface on the target plate's surface may be as great as 0.6 μsecond across a distance of 40 mm. In this case the shock waves in the target missile material will each be tilted 3° 26' with respect to the face of the target. The subsequent meeting of rarefaction waves would not be plane-parallel but would subtend an angle of 6° 52'. The closure of this angle will require 0.6 μsecond. By way of comparison, if the total angular deviation were only 1° 25', the velocity at which the missile and target make initial contact across their mutual face is exactly equal to the rate at which the compression wave moves through the copper. This will produce a two-dimensional situation. It is important to realize that the importance of plane impact will become more critical with decreasing velocity of impact.

SPECIMEN PREPARATION

23. Deformation of copper has been studied by many investigators (5), (6), (7), and (8) and the macroscopic processes by which copper deforms are well established, at least under conditions of static loading. Other investigators have studied deformation and fracture characteristics of materials under conditions of shock loading. Most of these investigations were concerned with gross macroscopic observations and scant attention was paid to microstructural changes. Also, test procedures employed usually produced non-planar shocks and grossly deformed test specimens. Investigations by Smith and by Rinehart and Pearson are notable exceptions. Both Smith (9) and Rinehart and Pearson (10) studied the microstructural changes which occur in shocked metals. Rinehart and Pearson made no particular efforts to control the wave shape in the specimen, while Smith used an explosive plane wave-generator which produced plane wave shock conditions.

24. The investigation discussed in this report studied the effect of essentially one-dimensional planar shock on copper in three different conditions. The composition of the copper used is presented in Table 1.

Table 1

Chemical Composition of Copper Material

Element	Percent by Weight
Cu	99.950
O_2	0.038
Sb	0.001
P	0.010

Specimens were machined from both 1-1/2-inch diameter bars in which the metal fiber is perpendicular to the faces of the specimen and 1/4-inch thick plate material in which the metal fiber is parallel to the faces of the specimen. The plate material was procured in the 1/4-hard and hard conditions; and bar material in the 1/4-hard condition. Annealed specimens from both bar and plate material were obtained by machining specimens from 1/4-hard condition material and subsequently

annealing at 1200°F for 1 hour under Argon. After annealing, both bar and plate material had an average grain size of approximately 0.056 mm.

25. Great care was taken in preparation of both specimen and missile pieces. The procedure which resulted in the greatest success is as follows:

Turning the test pieces to the approximate diameter.

Finishing faces either by flycutting or by turning on a lathe capable of maintaining a constant cutting rate across the face.

Lapping each face against a flat surface using wet papers through 400-grit SiC.

Obtaining finished faces which were extremely flat and with deviation from parallelism seldom exceeding 0° 0' 15".

26. Copper specimens of each condition were impacted over a range of impact velocities both above and below the velocity required to form a continuous spall crack (spall fracture), subsequently referred to as the critical impact velocity. At velocities just below the critical velocity, discontinuous spall cracks were observed. Arbitrarily these have been referred to as micro-spalls. Specimens impacted above the critical impact velocity were thicker due to the presence of the spall fracture. This increase in thickness provided a convenient method for determining the approximate critical impact velocity. Specimens which did not contain obvious spall fractures were microscopically examined for evidence of deformation and/or micro-spalls. Plastic deformation occurring in the specimens as a result of impacting was studied by examining polished metallographic specimens from virgin and impacted material and by microhardness testing. Spall fractures produced by impact were investigated by microscopically and macroscopically examining sections transverse to spall fracture surfaces, and by fractrographic examinations.

27. Results reported by other investigators show that deformations causing observed hardening in impacted materials occur on a scale not accessible to the optical microscope. For this reason microscopic examinations were not expected to yield very useful information on deformation processes except in spall fracture and micro-spall areas. Microhardness testing was therefore used to study hardening resulting from sub-microscopic deformation. In preparing specimens for microhardness tests it was necessary to grind on wet SiC papers and electropolish several times to remove effects from cutting which tended to mask the hardness changes produced by impacting.

INVESTIGATION RESULTS

Critical Spall Velocity.

28. Figures 9 and 10 show bulging as a function of impact velocity. Critical impact velocities determined from these figures and from the metallographic examination are:

>   Annealed bar -- 138 m/second
>
>   Annealed plate -- 61 m/second
>
>   1/4-hard plate -- 72 m/second
>
>   Hard plate -- 57 m/second.

From the above data it is apparent that the material condition, (i.e., annealed, 1/4-hard, or full hard) has little effect on the critical velocity to produce spall. However, it was found that fiber orientation has a very pronounced effect. Observe that the critical impact velocity for annealed plate was more than twice that for annealed bar material. In the plate material the fiber is aligned normal to and in the bar material parallel to the direction of impacting.

Observations of the Nature of Spall Fractures.

29. Spall fractures in copper plate and bar material differ greatly in appearance as the fractographs presented in Figure 11 show. Spall fractures in the plate material are cleavage fractures which show little attendant grain deformation. On the other hand spall fractures in the bar material are shear fractures with a large amount of grain deformation. Note the relatively severe grain deformation shown in the copper bar as compared with the copper plate spall fractures in photomicrographs presented in Figure 12.

30. In both materials the gross spall fractures formed perpendicular to the impacting direction. However, the orientation of the micro-spalls (Figures 13 and 14) was found to depend on the direction of the metal fiber. In the plate material micro-spalls formed perpendicular to and in the bar material parallel to the direction of impact. Micro-spalls were observed to be straight and parallel, and to form in a relatively narrow band. The location of the band is dependent on the test system geometry. The width of the band is considered to be dependent on the duration of the tension pulse. From Figure 13 the appearance and nature of the micro-spalls are observed to be similar regardless of the initial condition of the copper.
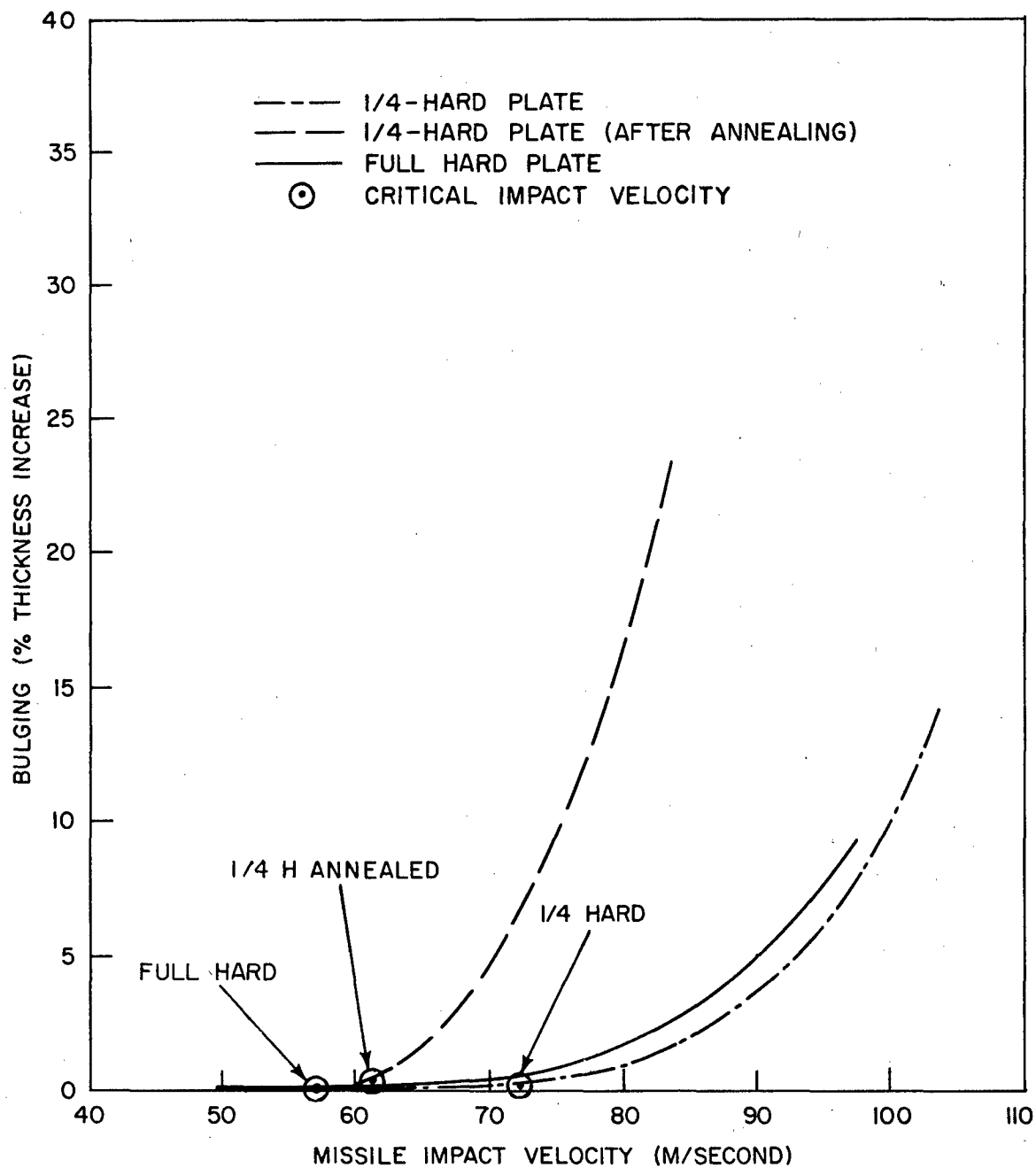
FIG. 9 BULGING VS IMPACT VELOCITY, COPPER PLATE MATERIAL

CRITICAL IMPACT VELOCITY

⊙ CRITICAL IMPACT VELOCITY

BULGING (% THICKNESS INCREASE)

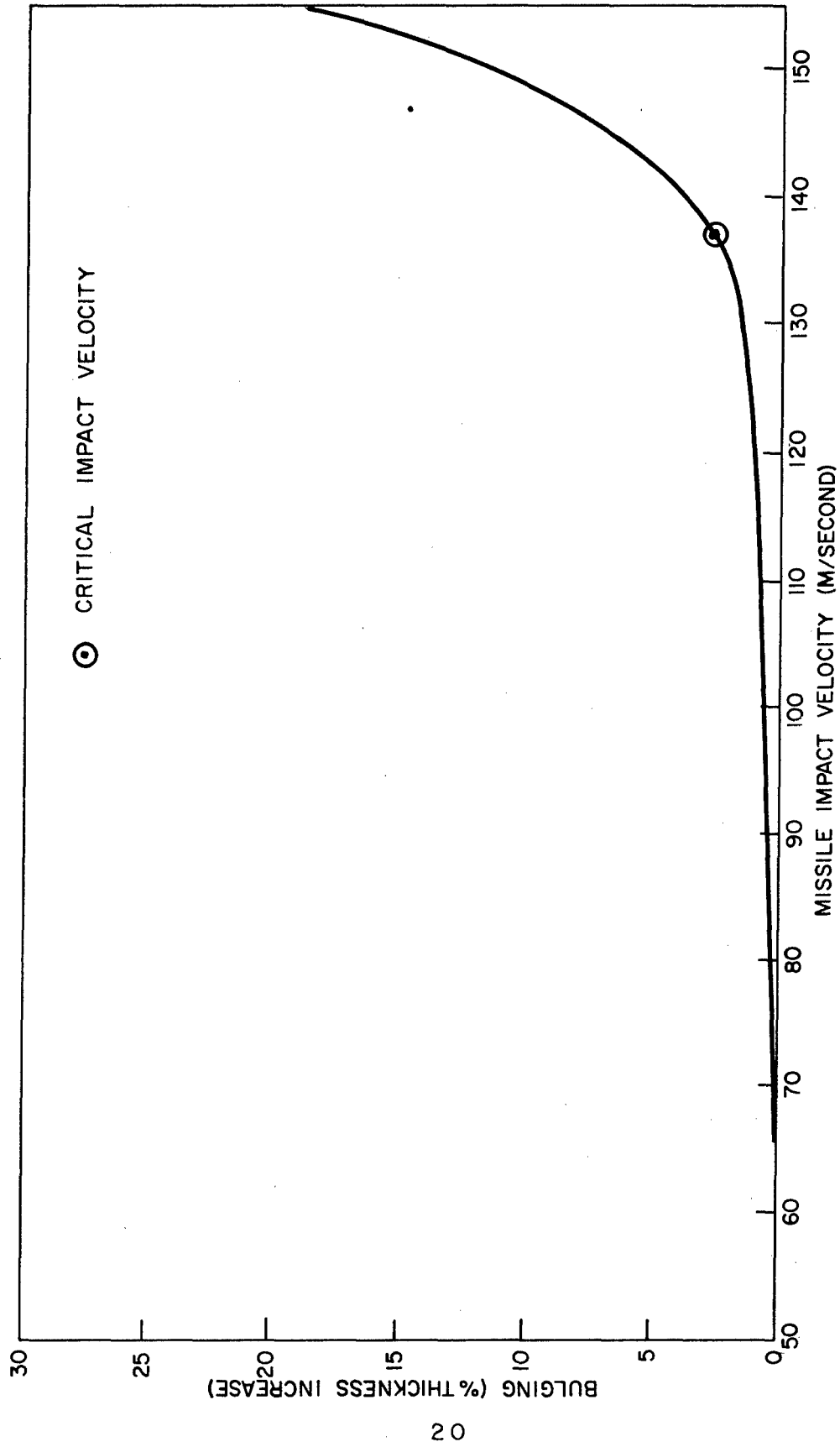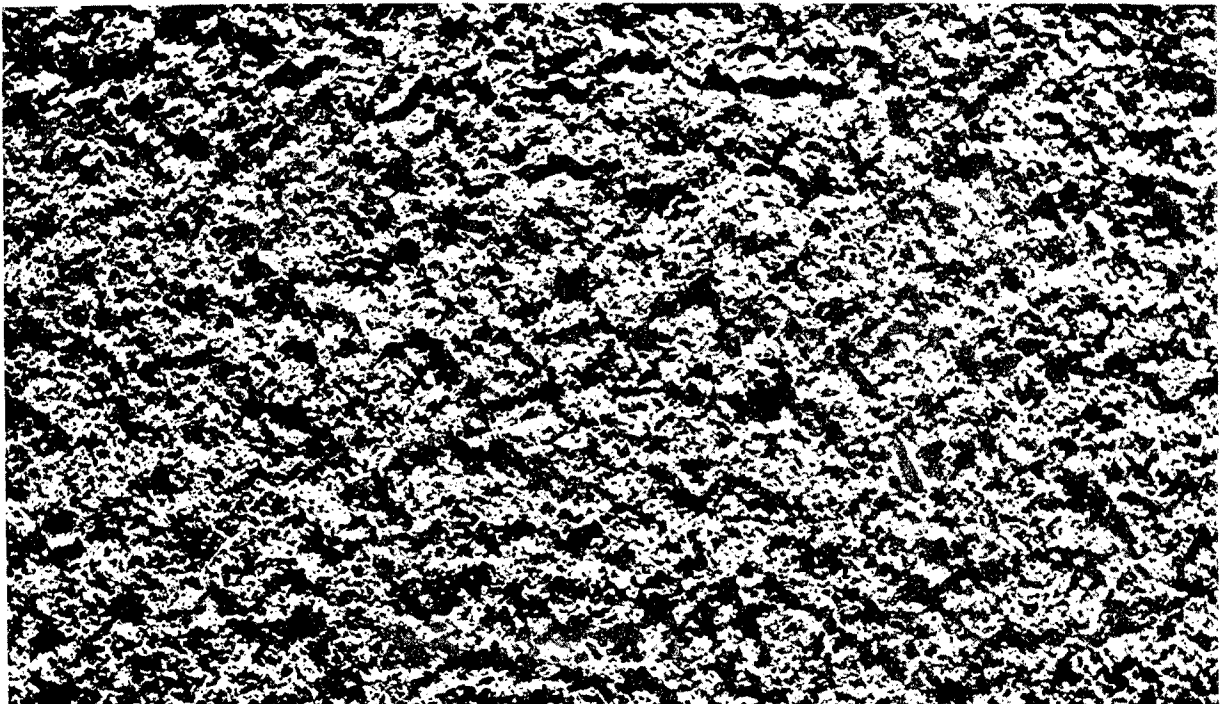MISSILE IMPACT VELOCITY (M/SECOND)

FIG. 10 BULGING VS IMPACT VELOCITY, COPPER BAR MATERIAL (ANNEALED)

20

FRACTURE SURFACE IN ANNEALED COPPER PLATE

FRACTURE SURFACE IN ANNEALED COPPER BAR.

|←——— 5mm ———→|

FIG. II FRACTOGRAPHS OF SPALL SURFACES

21

SPALLED COPPER PLATE
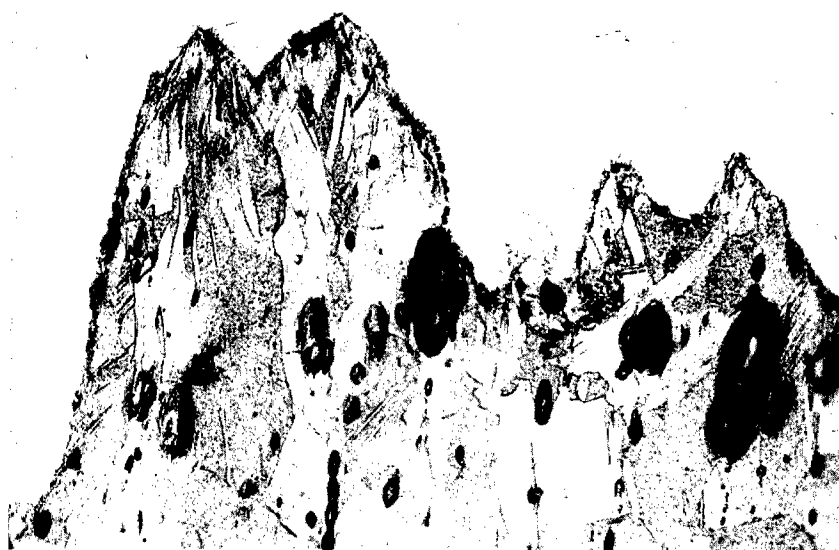
SPALLED COPPER BAR

|←——— 0.2mm ———→|

FIG. 12. MICROSTRUCTURES ADJACENT TO SPALL FRACTURES.
ETCHED IN 10% $(NH_4)_2 S_2 O_8$

IMPACT

ANNEALED COPPER PLATE
(IMPACT VELOCITY, 60 METERS PER SEC.)

1/4-HARD COPPER PLATE
(IMPACT VELOCITY, 70 METERS PER SEC.)

IMPACT

HARD COPPER PLATE
(IMPACT VELOCITY, 80 METERS PER SEC.)

|◄────── 1 cm ──────►|

FIG. 13. MICRO-SPALL IN COPPER PLATE SPECIMENS.
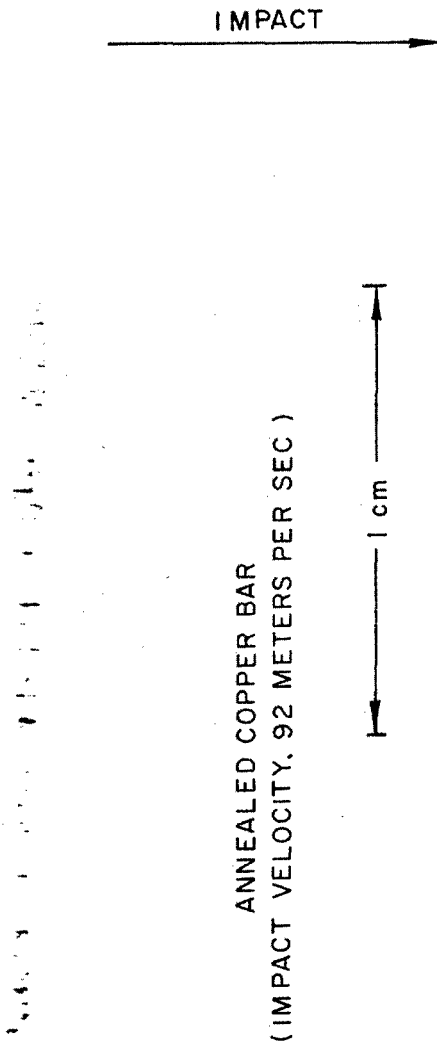
IMPACT →

ANNEALED COPPER BAR
(IMPACT VELOCITY, 92 METERS PER SEC)

⊢ 1 cm ⊣

FIG. 14 MICRO—SPALL IN COPPER BAR SPECIMEN

There is, however, an apparent dependence of the impacting velocity needed to produce a specific density of micro-spalls on the initial hardness. Harder material seemingly requires higher velocities to produce equivalent micro-spall densities.

31. Micro-spalls in both copper bar and plate material are transgranular, as can be seen in Figure 15.

32. Differences in the degree of deformation and appearance of spall fractures in bar and plate material are explained as follows:

In rolling copper, micro-cracks, inclusions, and other defects are aligned parallel to the direction of working. These aligned defects produce what is commonly called the metal fiber. Properties of fabricated copper, particularly mechanical properties such as tensile strength and ductility, are strongly dependent on the stress state with respect to the direction of the metal fiber, i.e., it is easier for cracks to form and propagate parallel to these aligned defects, (metal fiber), than perpendicular to them. Thus, the metal fiber can be considered to be composed of stringers of defects which form planes of weakness aligned in the direction of working.

Spall fractures in both copper bar and plate material form by propagation and/or joining of micro-spalls. In copper plate specimens, micro-spalls form first by cleavage. Completion of the fracture results from shear fracturing of material between the micro-spalls. Cleavage areas observed in copper plate spall fractures (Figure 11) are micro-spall surfaces.

Grain deformation observed at the fracture surfaces is confined to the shear fracture areas. The amount of deformation here depends principally on the amount of material separating the adjoining micro-spalls.

Spall fractures in copper bar material also occur in the manner described above. However, due to the orientations of the micro-spalls, no large cleavage areas are formed. The spall fractures are composed of shear fractures of the relatively large areas separating the micro-spalls. Thus, the spall fracture surfaces show extensive and severe grain deformation (see Figure 12).

33. Areas remote from spall fractures showed no microscopic evidence of plastic deformation. Typical microstructures of annealed copper plate specimens, as received and after impacting, are shown in Figure 16.

ANNEALED COPPER PLATE
(IMPACTED AT 60 METERS PER SEC.)
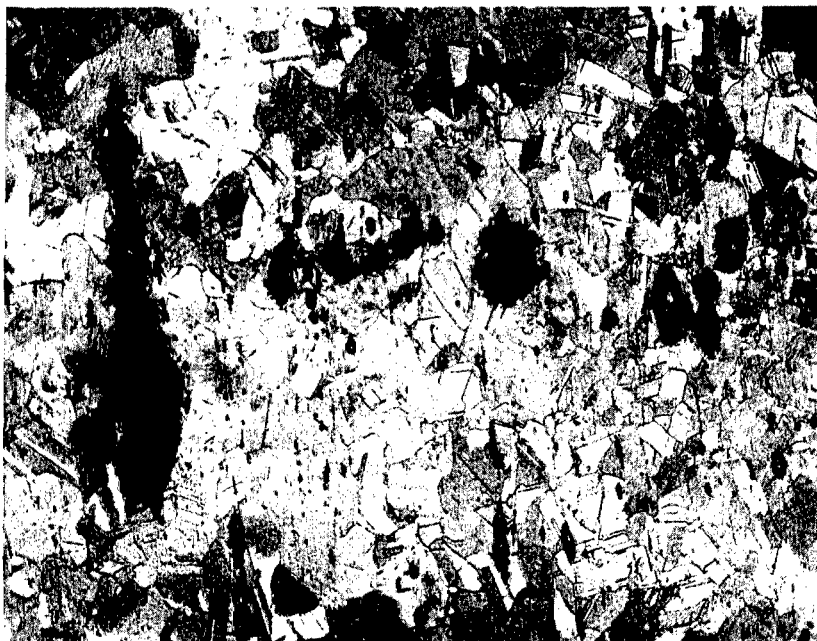
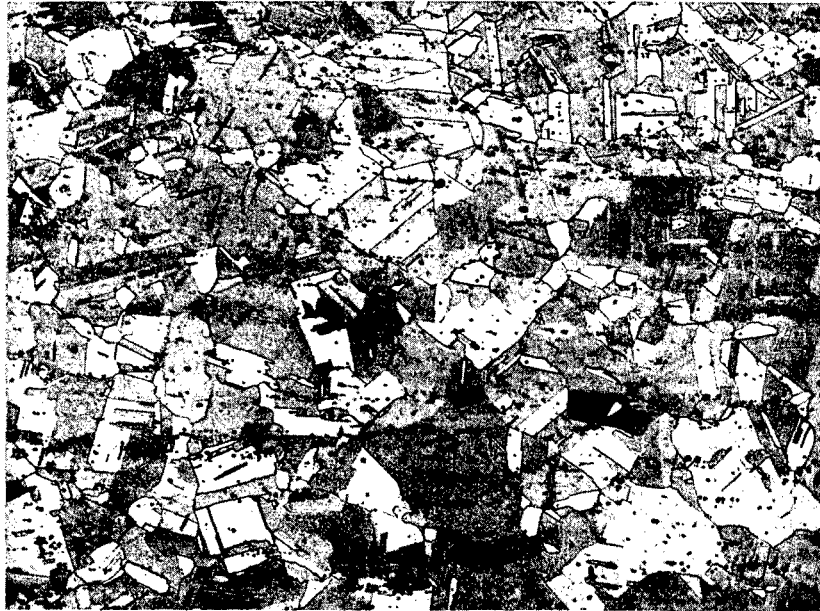ANNEALED COPPER BAR
(IMPACTED AT 90 METERS PER SEC.)

|←————0.5mm————→|

FIG. 15. MICROSTRUCTURES ADJACENT TO MICRO-SPALLS,
ETCHED IN 10% $(NH_4)_2S_2O_8$

IMPACT

26

VIRGIN ANNEALED CONDITION

AFTER IMPACT AT 60 METERS PER SEC.
(AREA REMOTE FROM SPALL)

IMPACT

|◄——————0.5mm——————►|

FIG. 16. MICROSTRUCTURES OF ANNEALED COPPER PLATE BEFORE
AND AFTER IMPACTING. ETCHED IN 10% $(NH_4)_2S_2O_8$

27

NOLTR 61-121

Hardening Produced by Impact.

34. Hardening which occurred as a result of high velocity impact was investigated by microhardness testing. Microhardness test results are presented in Figures 17 and 18. Figure 17 presents results of microhardness tests on a series of annealed copper plate specimens. Figure 18 presents a statistical summary of microhardness data for all materials investigated. In Figure 18 differences between means are a measure of the change in hardness with impacting velocity. The standard deviations are a measure of the significance of differences between means.

35. Microhardness curves for annealed copper plate (Figure 17) differed from curves for 1/4-hard and hard copper plate as follows:

> The microhardness traces for 1/4-hard copper plate were fairly flat, with less variation from edge to edge and a smaller increase in hardness at the fracture.

> The microhardness traces for hard copper showed more scatter, were virtually flat, and showed no trend of increasing hardness with increasing impact velocity.

In Figure 18 the slopes of lines which connect the mean microhardness values for the various specimens are a measure of the rate of increase in hardness with impact velocity. These slopes show that the degree of hardening is dependent on the initial condition of the copper. Lines connecting the mean microhardness value of annealed copper plate and bar specimens are parallel and nearly coincident in the velocity range for which data from both materials were available. Thus, the metal fiber orientation had no apparent effect on the overall hardening. Hardness data for 1/4-hard and annealed copper plate indicate hardness increases linearly with impact velocity up to 80 m/second, the maximum velocity applied to the plate material. However, data from annealed copper bar specimens impacted at higher velocities show a lower rate of hardness increase with impact velocity at impact velocities above 80 m/second.
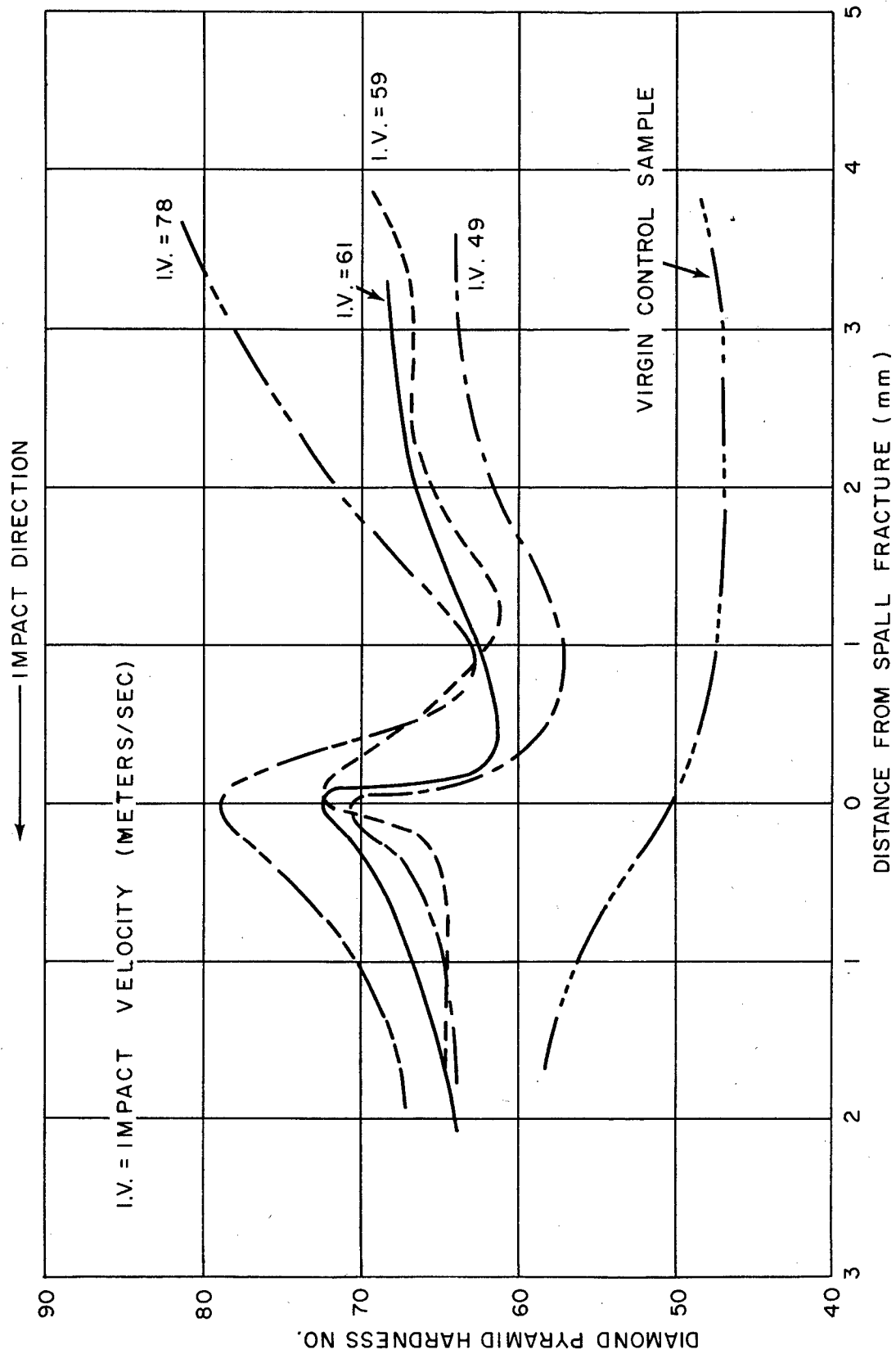
FIG. 17 MICROHARDNESS TRAVERSES ACROSS ANNEALED COPPER PLATE
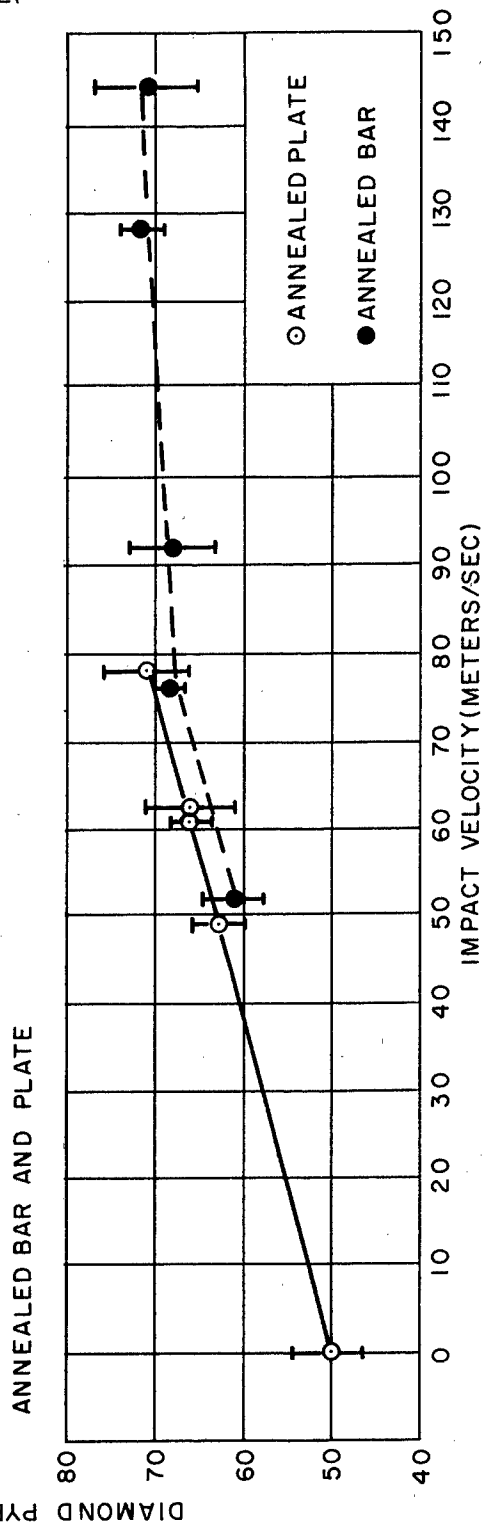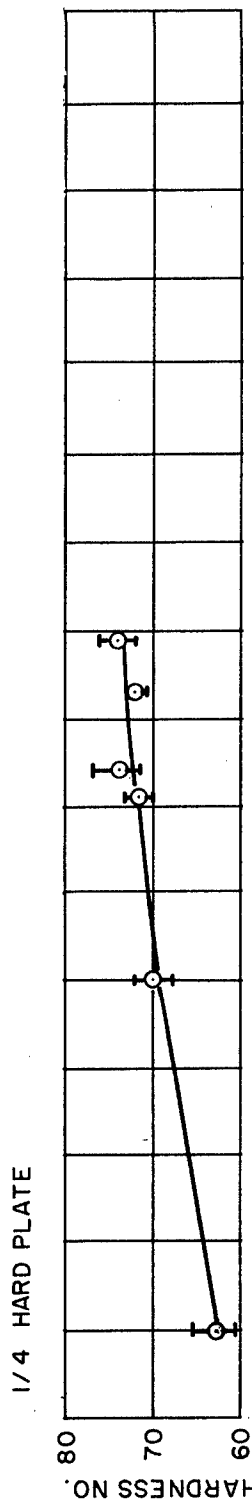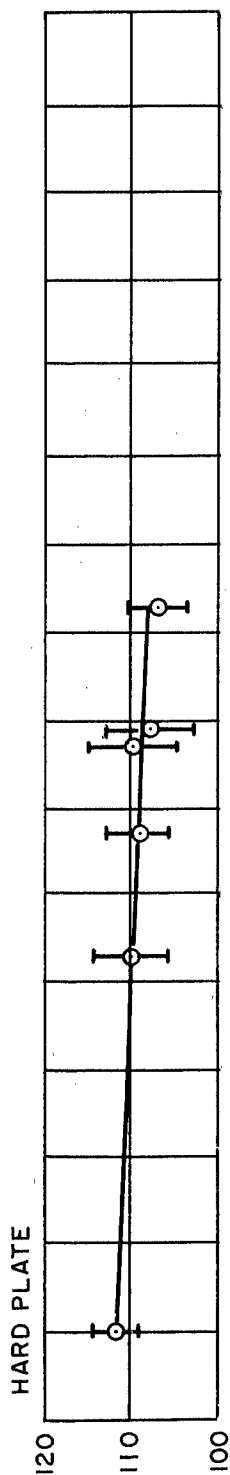FOR VARIOUS CONDITIONS OF IMPACT

FIG.18 AVERAGE MICROHARDNESS VALUES ACROSS COPPER SPECIMENS FOR VARIOUS IMPACT VELOCITIES. (MEAN VALUES AND ±I STANDARD DEVIATION INDICATED.)

SUMMARY AND DISCUSSION

36. The gas gun appears to be an appropriate tool for studying limiting conditions for the onset of spall in soft metals. In the experiment one obtains an accurate measure of impact conditions. One does not, however, obtain a measure of the unloading or tension conditions that hold at the time spall forms. It is therefore not possible to relate spall directly to a measured dynamic tension (negative pressure). As a first approximation to the tension it does not appear unreasonable to extrapolate shock equation of state data from the compressed region to the tension region since spall occurs at very low impact conditions. The tensions (negative pressures) predicted from material particle velocities are relatively independent of the nature of the extrapolation.

37. Formation of spall fractures in polycrystalline copper was found to depend largely on the alignment of microscopic and sub-microscopic flaws, (metal fiber), with respect to the direction of impact. Cleavage spall fractures occurred at relatively low impact velocities when the metal fiber was aligned normal to the direction of impact. Shear spall fractures, requiring higher impact velocities, occurred when the metal fiber and directions of impact were parallel. Initial material hardness (i.e., annealed, 1/4-hard, and hard) was found to have a relatively small effect on the critical impact velocity.

38. Copper specimens were observed to be hardened by impact. The degree of hardening as a function of impact velocity was found to be dependent on the initial hardness of the copper. No grain deformation or other microscopically observable structural changes accompanied the observed hardening.

39. Cottrell (11) explains the deformation of copper under conditions of high strain rates as follows:

> Dislocations in copper are gessile, that is, the stress field of a dislocation barrier exerts its effect primarily on the long range internal stress field of the dislocation.

> Under high rates of plastic strain when the applied stress (σ) exceeds the stress field of the obstacles (σ_1), dislocations in copper encounter no effective barriers until the velocity of the applied stress exceeds the speed of sound. Since this is the maximum speed at which shear stresses can be introduced into a material, the dislocations can move at the speed of the stress front where $\sigma \geq \sigma_1$.

31

Plastic strain associated with the movement and formation of dislocations prevents overloading of the material immediately back of the stress front. The maximum shear stress back of the shock front being limited to approximately σ_i. Thus, deformation of copper is relatively insensitive to changes in strain rate.

From these arguments and from experimental observations, deformation of copper at high strain rates is considered to occur by normal slip processes.

40. Investigation of high velocity deformation in copper single crystals is presently contemplated. Critical velocities to cause spall as a function of crystal orientations will be determined. Also, dislocation densities as a function of impacting velocity will be investigated by etch pit and microhardness techniques. Results of these investigations should provide information from which basic deformation processes can be studied.

REFERENCES

(1) M. H. Rice, R. G. McQueen, and J. M. Walsh, "Compression of Solids by Strong Shock Waves", Solid State Physics, Vol. 6, Ed. F. Seitz and D. Turnbull, (Academic Press, Inc., New York and London, 1958).

(2) G. Nahmani,"Experimental Investigation of Scabbing Produced in Mild Steel Plates by Plane Stress Waves", Colloque International sur les Ondes de Détonation, C.N.R.S., Gif-sur-Yvette (S.-&-O.) France, 28 aout - 2 septembre 1961.

(3) R. G. McQueen and S. P Marsh, "Equation of State for Nineteen Metallic Elements from Shock-Wave Measurements to Two Mega-Bars", J. Appl. Phys. 31, 1253 (1960).

(4) D. S. Hughes, L. E. Gourley, and M. F. Gourley, "Shock-Wave Compression of Iron and Bismuth", J. Appl. Phys. 32, 624 (1961).

(5) E. Schmid and W. Boas, "Kristallplastizitaet mit Besonderer Beruechsichtigung der Metalle", (Springer, Berlin, 1935); Plasticity of Crystals (translation from the German by F. A. Hughes & Co.)(F. A. Hughes & Co., London, 1950).

(6) T. H. Blewitt, R. R. Coltman, and J. K. Redman, "Low Temperature Deformation of Copper Single Crystals", J. Appl. Phys. 28, 651 (1957).

(7) W. A. Bachofen, A. J. Shaler, and B. B. Hundy, "Mechanical Anisotropy in Copper", Trans. ASM 46, 655 (1954).

(8) R. P. Carreker, Jr. and W. R. Hibbard, Jr., "Tensile Deformation of High-Purity Copper as a Function of Temperature, Strain Rate and Grain Size", Acta Metallurgia 1, 654, (1953).

(9) C. S. Smith, "Metallographic Studies of Metals After Explosive Shock", Trans. Metallurgical Soc. AIME 212, 574 (1958).

(10) J. S. Rinehart and J. Pearson, "Behavior of Metals Under Impulsive Loads", (American Society for Metals, Cleveland, 1954).

(11) A. H. Cottrell, "The Properties of Materials at High Rates of Strain", London Conference of Institute of Mechanical Engineers (IME, London, 1957), p. 18.

DISTRIBUTION

Copies

Director of Defense Research & Engineering
Department of Defense
Washington 25, D. C.   1

Chief, Bureau of Naval Weapons
Department of the Navy
Washington 25, D. C.
    DIS-32   1
    RRRE-5   1
    RUME-3   1
    RUME-32   1
    RMMO-5   1

Director, Special Projects Office
Department of the Navy
Washington 25, D. C.
    SP-20   4

Chief, Bureau of Ships
Department of the Navy
Washington 25, D. C.   2

Chief of Naval Research
Department of the Navy
Washington 25, D. C.
    Chemistry Branch   2

Commander
U. S. Naval Ordnance Test Station
China Lake, California
    Technical Library   2
    W. S. McEwen   1
    L. N. Cosner   1
    H. D. Mallory   1
    J. Pearson   1

Director, Naval Research Laboratory
Washington 25, D. C.
    Technical Information Section   1

Director
David Taylor Model Basin
Washington 7, D. C.   1
    A. H. Keil   1

	Copies
Commander Naval Air Development Center Johnsville, Pennsylvania Aviation Armament Laboratory	1
Commanding Officer U. S. Naval Ordnance Laboratory Corona, California	1
Commander U. S. Naval Weapons Laboratory Dahlgren, Virginia Technical Library	2
Commander U. S. Navy Electronics Laboratory San Diego, California	1
Commander Naval Air Missile Test Center Point Mugu, California	1
Chief, Defense Atomic Support Agency The Pentagon Washington 25, D. C.	2
Atomic Energy Commission Washington 25, D. C.	1

Office of Chief of Ordnance
Department of the Army
Washington 25, D. C.
    ORDTA
    ORDTB
    ORDTS
    ORDTT
    ORDTU
    ORDTX
	
	1
	1
	1
	1
	1
	1

Office of Chief of Engineers
Department of the Army
Washington, D. C.
    ENGNB
    ENGEB
	
	1
	1

Commanding Officer Office of Ordnance Research Box CM Duke Station Durham, North Carolina	1

Copies

Commanding Officer
Picatinny Arsenal
Dover, New Jersey
   Technical Information Section   1

Commanding Officer
Watertown Arsenal
Watertown, Massachusetts   1

Commanding General
Redstone Arsenal
Huntsville, Alabama
   For attn. of Rohm & Haas Co., Res. Div.   1
   Technical Library   1

Commanding General
Aberdeen Proving Ground
Aberdeen, Maryland
   Technical Library, Bldg. 313   1
   R. J. Eichelberger   1

Commanding General
Frankford Arsenal
Philadelphia 37, Pa.   1

Director, U. S. Bureau of Mines
Division of Explosives Technology
4800 Forbes Street
Pittsburgh 13, Pa.   1

Chief of Staff
U. S. Air Force
Washington 25, D. C.   1

Commander
Wright Air Development Center
Wright-Patterson Air Force Base
Dayton, Ohio
   WCEG   1

Headquarters, Air Proving Ground Center
U. S. Air Force, ARDC
Eglin Air Force Base, Florida
   Attn: Technical Library (PGTRI)   1

                                                              Copies

Commander
Air Research & Development Command
Andrews Air Force Base
Washington 25, D. C.
     RDT   1

Commander
Air Force Special Weapons Center
Kirtland Air Force Base
Albuquerque, New Mexico   1

National Aeronautics and Space Administration
1512 H Street, N. W.
Washington 25, D. C.   1

National Aeronautics & Space Administration
Goddard Space Flight Center
Greenbelt, Maryland   1

National Aeronautics & Space Administration
Lewis Research Center
21,000 Brookpark Road
Cleveland 35, Ohio
     Library   1

National Aeronautics & Space Administration
Ames Research Center
Moffett Field, California   1

University of California
Lawrence Radiation Laboratory
P. O. Box 808
Livermore, California
     Technical Information Division   1

Sandia Corporation
P. O. Box 5400
Albuquerque, New Mexico   1

Los Alamos Scientific Laboratory
P. O. Box 1663
Los Alamos, New Mexico
     Library   1

Sandia Corporation
P. O. Box 969
Livermore, California   1

	Copies
Armed Services Technical Information Agency Arlington Hall Station Arlington 12, Virginia	10
Office of Technical Services Department of Commerce Washington 25, D. C.	100
NOL Representative in the United Kingdom (W. B. Coffman) U. S. Naval Attache, Box 49 Navy 100, Fleet Post Office New York, New York	1
Director, Stanford Research Institute Stanford, California The Poulter Laboratories	2
Director, Applied Physics Laboratory, JHU 8621 Georgia Avenue Silver Spring, Maryland	1
Arthur D. Little, Inc. 30 Memorial Drive, Library Cambridge 42, Mass. (V. Vabri)	1
Explosives Research Group University of Utah Salt Lake City, Utah	1
Armour Research Foundation Illinois Institute of Technology 10 W. 35th Street, Chicago 16, Ill.	1
Aerojet-General Corporation Downey, California Dr. L. Zernow	1
Colorado School of Mines Golden, Colorado Dr. J. S. Rinehart	1

Naval Ordnance Laboratory, White Oak, Md.
(NOL technical report 61-121)
SPALL STUDIES IN COPPER, by R.A. Plauson and others. 28 Dec. 1961. 33p. charts, diagrs. Task FR-52. UNCLASSIFIED
A gas gun system for use in studying one-dimensional spall conditions in thin metal plates is described. This gun is capable of producing well controlled plane impact of a "missile" disc 1.69 inch in diameter on a "target" disc of adjustable diameter at velocities up to 150 meters per second. Missile and target thicknesses can be varied as required in the experiments.

Abstract card is unclassified

1. Guns, Gas
2. Copper - Spalling
I. Title
II. Plauson, Richard A.
III. Project